The modulatory role of pre-SMA in speed-accuracy tradeoff

Neuropsychologia 109 (2018) 255–261

Contents lists available at ScienceDirect

Neuropsychologia

journal homepage: www.elsevier.com/locate/neuropsychologia

The modulatory role of pre-SMA in speed-accuracy tradeoff: A bi-directional TMS study

Dilara Berkay[a,b], Hale Yapıcı Eser[b,c], Alexander T. Sack[d], Yusuf Özgür Çakmak[e], Fuat Balcı[a,b,*,1]

[a] Department of Psychology, Koç University, Istanbul, Turkey
[b] Research Center for Translational Medicine, Koç University, Istanbul, Turkey
[c] Department of Psychiatry, Koç University, School of Medicine, Istanbul, Turkey
[d] Department of Cognitive Neuroscience, Maastricht University, Maastricht, The Netherlands
[e] Department of Anatomy, University of Otago, Dunedin, New Zealand

ARTICLE INFO

Keywords:
Speed accuracy tradeoff
Presupplementary motor area
Decision making
Drift diffusion model
Theta burst stimulation

ABSTRACT

Many perceptual decisions are inevitably subject to the tradeoff between speed and accuracy of choices (SAT). Sequential sampling models attribute this ubiquitous relation to random noise in the sensory evidence accumulation process, and assume that SAT is adaptively modulated by altering the decision thresholds at which the level of integrated evidence should reach for making a choice. Although, neuroimaging studies have shown a relationship between right presupplementary motor area (pre-SMA) activity and threshold setting, only a limited number of brain stimulation studies aimed at establishing the causal link, results of which were inconsistent. Additionally, these studies were limited in scope as they only examined the effect of pre-SMA activity unidirectionally through experimentally inhibiting the neural activity in this region. The current study aims to investigate the predictions of the striatal theory of SAT by experimentally assessing the modulatory effect of right pre-SMA on threshold setting bi-directionally. To this end, we applied both offline inhibition and excitation to the right pre-SMA utilizing transcranial magnetic stimulation in a within-subjects design and tested participants on a Random Dot Motion Task. Decision thresholds were estimated using the Hierarchical Drift Diffusion Model. Findings of our planned comparisons showed that right pre-SMA inhibition leads to significantly higher, whereas right pre-SMA excitation leads to significantly lower thresholds without showing any effects on the evidence integration process itself.

1. Introduction

In our daily life, we encounter numerous occasions that require us to make a choice between various options such as deciding which of the two lines at the supermarket cashier runs faster (perceptual judgments). Since the sensory information and/or its processing are subject to noise, making an adaptive choice typically requires accumulating some evidence. Accumulating more evidence will lead to more accurate but also slower decisions, whereas accumulating less evidence will lead to faster but also less accurate decisions. This is referred to as the speed-accuracy tradeoff (SAT; Schouten and Bekker, 1967; Wickelgren, 1977) and necessitates balancing how fast and accurate one aims to be in their decisions for maximizing the reward rate.

Data gathered from decision making experiments reveal information about response time (RT) distributions for both correct and incorrect responses such as their mean, shape, and skewness (Voss et al., 2013). When the analyses are based on accuracy or RT data in an isolated fashion, this rich information in RT distributions is ignored and/or reduced to convenient but less informative descriptives.

In order to study SAT in two-alternative forced choice (2AFC) tasks in a fashion that sheds light on the underlying latent decision process, it is essential to take account of accuracy and RT data in a unified fashion by using computational models. The Drift Diffusion Model (DDM) constitutes an example to these decision theoretic approaches (Bogacz, 2007; Gold and Shadlen, 2007; Ratcliff, 1978; Ratcliff and McKoon, 2008; Ratcliff and Rouder, 1998; Smith and Ratcliff, 2004; Voss et al., 2013). According to DDM, decisions are made based on a noisy evidence accumulation process. The sensory evidence starts to accumulate from an initial belief state (starting point) and moves in a decision area bounded by two attractors (decision thresholds for correct and incorrect options). This accumulation process is represented by a decision variable, which on average moves towards the threshold that is supported

* Correspondence to: Department of Psychology, Koç University, Rumelifeneri Yolu, Sarıyer, 34450 Istanbul, Turkey.
E-mail address: fbalci@ku.edu.tr (F. Balcı).
[1] https://tmdmlab.ku.edu.tr/.

https://doi.org/10.1016/j.neuropsychologia.2017.12.031
Received 19 August 2017; Received in revised form 29 November 2017; Accepted 15 December 2017
Available online 20 December 2017
0028-3932/

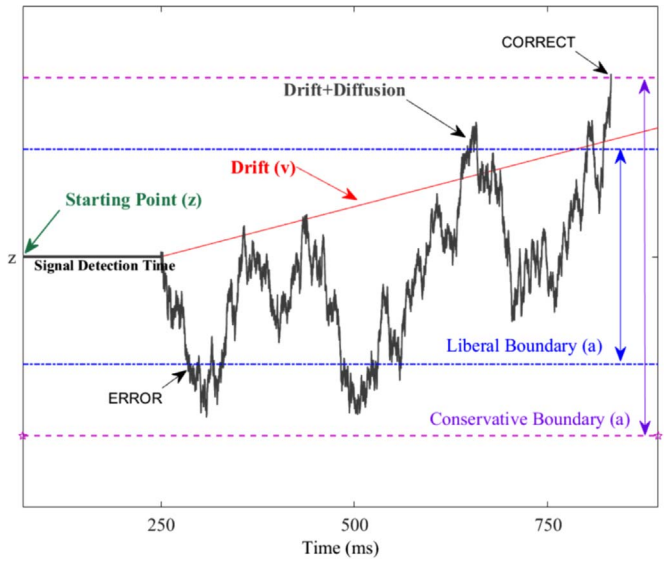

Fig. 1. A schematic for the drift-diffusion model where a sample path within a trial is illustrated for conservative (purple horizontal dashed lines) and liberal (blue horizontal dashed-dotted lines) boundary setting conditions. In the liberal boundary setting condition, the decision process takes less time but hits the incorrect (lower) boundary, whereas in the conservative boundary setting condition, the decision variable hits the correct (upper) boundary at the cost of a longer decision time.

by the sensory evidence. Once the accumulated evidence hits one of these thresholds, the agent makes the corresponding choice (Ratcliff and Rouder, 1998; Forstmann et al., 2015; Ratcliff, 1978; Shadlen and Newsome, 2001; Ratcliff and McKoon, 2008; Bogacz et al., 2010).

Based on the DDM framework, the latent decision process is represented by four key parameters (see Fig. 1). The first parameter is drift-rate (v), which represents the average amount of evidence accumulated in unit time. This parameter is affected by the quality of the sensory evidence (lower drift-rate for harder tasks). The second parameter is the boundary separation (a), which determines the amount of evidence required to make a choice. The third parameter, starting point (z), indicates where the decision-maker starts to accumulate evidence in the decision area bounded by two decision thresholds. Lastly, non-decision time reflects the RT components that are not related to the decision process.

Within the DDM framework, how high the decision thresholds (boundary/2) are set directly determines the SAT. As described above, the sensory/perceptual processing as well as the sensory evidence itself is subject to noise, which is reflected in the variability of the path that the decision variable travels over time. It is due to this variability that a decision variable with a drift in the direction of one of the decision thresholds can still hit the incorrect threshold, leading to the choice of the incorrect option. When the threshold is set high (conservative), the probability of hitting the incorrect threshold decreases as the noise averages out over the decision process. Thus, higher threshold setting increases accuracy at the cost of longer RTs. Setting a lower threshold (liberal), on the other hand, means that less evidence will be needed to make a decision, leading to faster but more error-prone responses (see Fig. 1). Depending on the task requirements, one can favor speed over accuracy or vice versa by modulating the decision thresholds in opposite directions.

There are an ample number of studies that have focused on SAT at the level of the behavioral outputs and the computational principles that lead to it (Ratcliff and Smith, 2004; Wagenmakers et al., 2008). In contrast, the number of studies that have investigated the neural mechanisms of this adaptive modulation of SAT is limited (Herz et al., 2017; for review see Bogacz et al., 2010). Nonetheless, the available neurocomputational and empirical evidence of these studies strongly indicate a primary role of the cortico-striatal network in adaptive decision-threshold modulation (e.g., neurocomputational studies: Bogacz and Gurney, 2007; Frank, 2006; Gurney et al., 2004; Lo and Wang, 2006; empirical studies: Tosun et al., 2017; Georgiev et al., 2016). According to this theory, when the task demands emphasize speed over accuracy, striatal activity is increased via excitatory neural input from pre-SMA, which in turn weakens the inhibitory effect of basal-ganglia on the motor execution-related cortical areas leading to faster choices (Bogacz et al., 2010; Forstmann et al., 2008). A substantial number of neuroimaging studies that showed increased pre-SMA and striatal activity when speed was emphasized in 2AFC tasks support the involvement of this pathway in threshold modulation (Ding and Gold, 2010; Forstmann et al., 2010; Ivanoff et al., 2008; Mansfield et al., 2011; van Maanen et al., 2011; van Veen et al., 2008; Wenzlaff et al., 2011). Addressing this relation more directly, other studies demonstrated a relation between decision-threshold modulation, pre-SMA, and striatal activity (Forstmann et al., 2008; Mansfield et al., 2011) as well as a relation between decision-threshold modulation efficacy and pre-SMA-striatal connectivity (Forstmann et al., 2010).

In addition to these correlational findings, to our knowledge, only three brain stimulation studies have been conducted to elucidate the role of pre-SMA in decision-threshold modulation. In these studies, brain stimulation was combined with computational modeling (for earlier work combining TMS with computational modeling see Kadosh et al., 2010; Soto et al., 2012). This approach provides valuable insights into the source of the behavioral effects observed after the modulation of the activity in a specific brain region and thus allows one to derive more precise conclusions regarding the role of the target brain region (Hartwigsen et al., 2015; Romei et al., 2016). In one of these three studies, de Hollander et al. (2016) applied anodal transcranial direct current stimulation (tDCS) to modulate the activity of pre-SMA prior to testing participants on a perceptual 2AFC task where either speed or accuracy was emphasized in a given trial. In three independent studies, no effect of anodal tDCS of pre-SMA on threshold modulation (or on other core DDM parameters) was found. The other two studies used transcranial magnetic stimulation (TMS) to modulate the pre-SMA activity. From these studies, the findings of Georgiev et al. (2016) were counter-intuitive since they indicated that the inhibition of pre-SMA by continuous theta burst stimulation (cTBS) led to lower thresholds when accuracy was emphasized in the task. In contrast to Georgiev et al.'s findings and consistent with the cortico-striatal theory of decision-threshold modulation, Tosun et al. (2017) found accuracy bias, increased decision thresholds, and increased drift-rates (with no differential speed or accuracy emphasis) as a result of the inhibition of pre-SMA after cTBS.

The cortico-striatal theory of decision-threshold modulation predicts lower decision thresholds with higher pre-SMA activity and higher decision thresholds with lower pre-SMA activity. Even though the predictions of this model are bi-directional, no TMS study until hitherto ever tested this modulatory bi-directional effect using opposing stimulation protocols over pre-SMA in the same participants. The current study had two primary aims: a) replicating our previous findings regarding the increased decision thresholds with inhibition of right pre-SMA using more precise localization based on structural MRI-guided neuronavigation, and b) testing the directional predictions regarding the effect of excitation in addition to inhibition of right pre-SMA on decision-threshold modulation.

2. Methods

2.1. Participants

The minimum number of participants required to detect behavioral effects of TMS using group Talairach coordinates has been shown to be 13 (Sack et al., 2009). Based on this estimate, seventeen right-handed healthy volunteers (12 females) aged between 21 and 29 years (M = 25.27, SD = 2.49) were recruited for the study. A pre-experimental

health form was used to screen for contraindications of TMS and magnetic resonance imaging (MRI). Two participants were excluded from the study due to a family history of epilepsy. In order to foster task engagement, participants were told that they could receive monetary reward up to 110 TRY depending on their task performance, but all were paid 110 TRY at the end of the study. The study was approved by the institutional review board at Koç University and all participants provided written consent for each procedure prior to experimentation.

2.2. Apparatus

Structural brain images were obtained on a Siemens 3T scanner using a 16-channel array head coil. For brain stimulation, a Magstim Super Rapid^2 magnetic stimulator (70-mm figure-of-eight coil) was used. In order to localize target brain regions in real time, an ultrasound-based tracking system (CMS20; Zebris Medical GmbH, Germany) was used along with the TMS Neuronavigator software (Brain Innovation BV, The Netherlands). All participants were tested on a Macintosh computer with a 21.5-in. monitor. Noise cancelling headphones were used for auditory feedback and responses were collected via a mechanical keyboard.

2.3. Random Dot Motion (RDM) discrimination task

All stimuli were presented using the Psychtoolbox extension (Brainard, 1997; Pelli, 1997) in Matlab utilizing the SnowDots framework developed by Joshua Gold at the University of Pennsylvania. In the RDM discrimination task, participants were presented with a set of moving white dots on a black background. The dots were presented within a 3-in. circular space centered on the screen (see Gold and Shadlen, 2001). On each trial, a predetermined portion of the dots coherently moved towards either left or right with equal probability and the remaining dots were randomly displaced at each time step. Participants were asked to report the direction of the coherent motion by pressing 'Z' for left and 'M' for right. An auditory tone followed correct responses. We used a response-to-stimulus interval (RSI) sampled from a left truncated exponential distribution with a mean of 2-s and a lower bound of 1-s. Each correct response was worth 4-kuruş and there was no penalty for incorrect responses. Responses emitted during the RSI or within the first 100-ms of the stimulus onset were considered as premature/anticipatory responses and were penalized by a 1-s timeout which started after a buzzing sound (.1% of all trials). The cumulative number of correct responses was presented after every 10 trials.

Each session was comprised of nine 4-min test blocks of free-response (FR) RDM task with no deadline for responding and two 2-min signal detection blocks (SD - not analyzed here due to long delay since stimulation). Participants were instructed to respond as quickly and accurately as possible in the FR blocks. The coherence level, that is, the percentage of dots showing coherent motion, was set at 8%. Before the first session, participants completed an additional 4-min practice block of FR trials with 16% coherence. Participants could take a break of up to 4-min between blocks. The task lasted approximately 45-min.

2.4. Design and procedure

A repeated-measures design was used in the study. Before the experimental sessions started, brain images for all participants were obtained to be used for the localization of the target brain regions. In the first (practice) session, participants completed the RDM task without any experimental manipulation. In the following three (test) sessions, they completed the same task after pre-SMA inhibition, pre-SMA excitation, and vertex excitation/inhibition (control condition) in a counterbalanced order. In half of the participants we inhibited the vertex whereas in the other half we used excitation for the control condition.

2.4.1. Structural MRI scan and neuronavigation

Structural MRI was performed on a 3T scanner (Siemens Skyra, Erlangen, Germany). A total of 176 coronal slices were acquired (TR = 1900 ms, TE = 2.52 ms, FOV = 250 mm, 1 mm slice thickness, 256 × 256 matrix size, 1 × 1 × 1 voxel size and 1 ms excitation time). In order to localize target brain regions in real time, an ultrasound-based tracking system (CMS20; Zebris Medical GmbH, Germany) was used along with the TMS Neuronavigator software (Brain Innovation BV, The Netherlands). Target brain region was determined as pre-SMA (Talairach coordinates: x = 4, y = 5, z = 45).

2.4.2. rTMS protocol

In the experiment, we used theta burst stimulation (TBS) for modulating brain activity, as this method provides some advantages over the traditional repetitive stimulation methods. Specifically, administering TBS takes a very short time and it has an after-effect that far exceeds that of the traditional repetitive mode (Huang et al., 2005). In this protocol, each burst consists of three pulses given at 50 Hz and is repeated every 200 ms (5 Hz). We used two different patterns of TBS, namely continuous TBS (cTBS) and intermittent TBS (iTBS), in order to establish inhibitory and excitatory effects, respectively. In cTBS a 40 s uninterrupted train of TBS was applied (600 pulses). This paradigm has been shown to have an inhibitory after-effect of up to 60 min. For iTBS, a 2 s train of TBS was applied with 8-second intervals between each train for 190 s (600 pulses). The excitatory after-effect of iTBS lasts approximately 15–20 min.

The intensity for TBS was set individually at 80% of active motor threshold (AMT). Participants were asked to clench their hands while finding AMT. AMT was determined as the minimum stimulator output that, when applied to motor cortex, induces a motor response in the contralateral hand muscle in at least five out of ten trials. AMT was measured at the beginning of the behavioral (first) session and the same threshold was used for all TMS sessions.

3. Data analysis

The units of analysis were the accuracy and RT data obtained from the first four blocks of each session, which was decided on prior to any data analysis during study design. We used only the first four blocks since the after-effects of iTBS does not exceed 20-min. The same rule was also applied to the data collected from cTBS and vertex stimulation sessions in order to avoid any confounds due to differential fatigue and boredom between the iTBS, cTBS, and vertex sessions. In order to compare the change in RT and accuracy data, we conducted one-way repeated-measures ANOVAs. We also conducted Bayesian ANOVAs to reveal the odds in favor of the null hypothesis.

In order to evaluate the changes in latent decision processes, we used hierarchical Bayesian estimation method of DDM parameters (HDDM) (Wiecki et al., 2013). We used HDDMRegressor class in order to estimate within-subject effects. This method provides a more powerful way to detect differences in parameter estimates across different experimental conditions by constraining the individual fits by the group distribution. In Bayesian estimation method, parameter estimates are quantified in the form of posterior distributions using Markov chain Monte-Carlo (MCMC) sampling method. Using this framework allows one to test whether there is a significant difference in the parameter estimates across conditions directly on the posterior distributions instead of having to rely on the frequentist statistics. Specifically, we computed the posterior distributions for the difference between stimulation conditions for each parameter estimate. For significance testing, we examined the proportion of the posterior distribution that did not cross the value 0. When more than 95% of the difference between two posterior distributions was either higher or lower than 0, we concluded that there was a significant effect. Each posterior distribution has a normal, or truncated normal distribution depending on the bounds centered around the group mean. Prior distributions were based

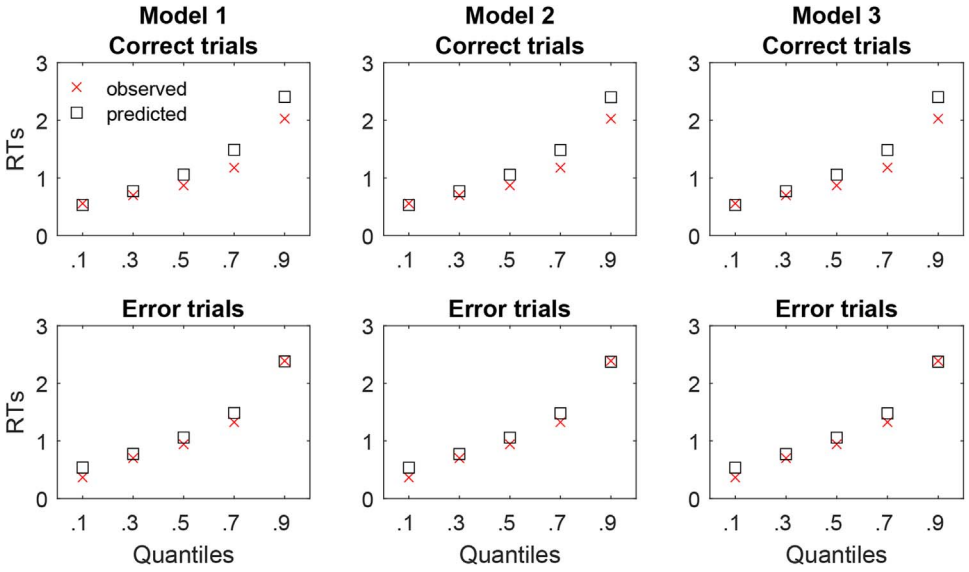

Fig. 2. Observed (red crosses) and predicted (black open squares) RTs for .1, .3, .5, .7, and .9 quantiles separately for correct (top row) and error trials (bottom row) for three different models (columns).

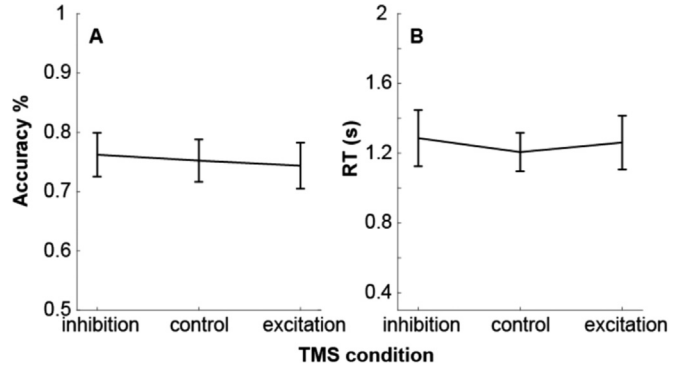

Fig. 3. Average accuracy levels (A) and response times (B) for different TMS conditions.

on previous 23 studies reporting best-fitting DDM parameters for a variety of decision-making tasks (for details see Matzke and Wagenmakers, 2009; Wiecki et al., 2013). Since within-subject data are slower to converge compared to between-subjects data, we used a higher sampling rate by drawing 10000 samples from the posterior and discarding the first 1000 as burn-in. We assessed whether the MCMC chains successfully converged by calculating Gelman-Rubin R statistic based on five separate runs of each model. This statistic gives the ratio between within- and between-chain variances. The value we obtained for each model was lower than the criterion of 1.02, which indicates successful convergence (Wiecki et al., 2013). In order to examine whether the models could successfully reproduce the observed data, we ran posterior predictive checks. The results indicated that for all models (described below), the observed data were within 95% credible interval of the data predicted by the models (see Fig. 2).

In model fitting, it is important to have a theory-driven approach since one can end up with the problem of overfitting without a prior hypothesis. For this reason, we adopted a theory-driven approach to determine which DDM parameters to vary and which ones to keep fixed across conditions. As our main hypothesis was that pre-SMA activity will modulate threshold setting, we allowed this parameter to vary across conditions. However, as our previous study (Tosun et al., 2017) indicated a change also in drift-rate as a result of the inhibition of pre-SMA with cTBS, we fitted a second model where both threshold and drift-rate were allowed to vary across conditions. Additionally, even though it was not part of our prior hypotheses, we were interested in testing if the results regarding threshold change based on the first two models survived a more complex model and thus fitted a third model where non-decision time was varied in addition to threshold and drift-rate. Lastly, we fit a null model where all parameters were fixed, in order to compare the other models against. The inter-trial variability parameters were not included in any of the models. Model comparison statistics did not favor the null model (DIC = 30647) over any of the other models. Model1 (DIC = 30616) provided a better fit than Model2 (DIC = 30618), although the difference was not significant. Despite that Model3 provided a better fit than both Model1 and Model2 (DIC = 30601), results based on Model3 should be interpreted by caution due to its exploratory nature.

4. Results

4.1. RT and accuracy comparisons

We first analyzed these behavioral outputs in isolation. Results of these analyses indicated that accuracy levels did not change across conditions (see Fig. 3), $F(2,28) = .19$, $p = .83$. The Bayesian analyses revealed that the odds were 4.86:1 (strong evidence; Raftery, 1995) in favor of the null hypothesis that accuracy level did not differ across conditions. The results also showed that RTs did not differ, $F(2,28) = .33$, $p = .72$ across conditions (5.24:1 in favor of null hypothesis).

4.2. Effects on the latent decision process

In order to investigate the effect of stimulation condition on the latent decision processes, we fit three different hierarchical DDMs outlined above. The models differed in terms of the parameters allowed to vary across experimental conditions.

Fig. 4 illustrates the difference between pre-SMA inhibition/excitation and vertex stimulation conditions for each parameter in Model1 (A), Model2 (B), and Model3 (C). For Model 1, in which we only allowed the threshold parameter to vary across different conditions, we found that decision thresholds were significantly higher in pre-SMA inhibition condition than the vertex stimulation condition ($p(a_{\text{inhibition}} > a_{\text{control}}) = .9993$), whereas they were significantly lower in pre-SMA excitation condition than the vertex stimulation condition ($p(a_{\text{excitation}} < a_{\text{control}}) = .9938$). The same findings regarding decision thresholds held for Model 2, in which threshold and drift-rate were allowed to vary across different conditions ($p(a_{\text{inhibition}} > a_{\text{control}}) = .9998$; $p(a_{\text{excitation}} < a_{\text{control}}) = .9966$). There were no significant differences in drift-rates between pre-SMA inhibition vs. vertex stimulation ($p(v_{\text{inhibition}} > v_{\text{control}}) = .9288$) or pre-SMA excitation vs. vertex stimulation ($p(v_{\text{excitation}} > v_{\text{control}}) = .5131$) conditions.

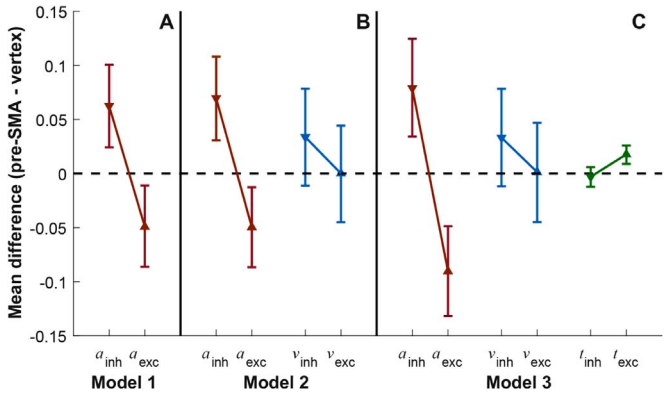

Fig. 4. Mean difference in the threshold (a; red), drift rate (v; blue), and non-decision time (t; green) parameters between pre-SMA inhibition and control and pre-SMA excitation and control conditions for Model 1 (A), Model 2 (B), and Model 3 (C). Error bars indicate 95% credible intervals. Note that positive differences indicate higher values in the pre-SMA compared with vertex stimulation conditions, whereas negative values indicate lower values in pre-SMA compared with vertex stimulation conditions.

Finally, we fit a third model to the data allowing decision threshold, drift-rate, and non-decision time to vary across different conditions, in order to explore if the observed threshold differences would survive this more complex model. In Model3 (included for exploratory purposes) we found the same results with Model1 and Model2 regarding both decision thresholds ($p(a_{\text{inhibition}} > a_{\text{control}}) = .9998$; $p(a_{\text{excitation}} < a_{\text{control}}) = 1$) and drift-rates ($p(v_{\text{inhibition}} > v_{\text{control}}) = .9248$; $p(v_{\text{excitation}} < v_{\text{control}}) = .5275$). Additionally, we found a difference in non-decision times across conditions. Specifically, non-decision time was significantly higher in the pre-SMA excitation compared to the control condition ($p(t_{\text{excitation}} > t_{\text{control}}) = 1$); whereas there was no difference between pre-SMA inhibition and control conditions ($p(t_{\text{inhibition}} < t_{\text{control}}) = .7477$).

We originally fit the data collected from the first four blocks in all three conditions as the expected effect of iTBS is known to span the corresponding test duration and we wanted the data collected from other conditions (cTBS and vertex) to be comparable to iTBS conditions in all other respects. For completeness, we also report the results gathered based on the data in the remaining test blocks to test the robustness of our findings.

Similar to our primary results reported above, the results obtained from the last five blocks revealed that there was no significant difference in accuracy levels ($F(2,28) = .96$, $p = .39$) or RTs ($F(2,28) = .06$, $p = .94$). As expected based on the duration of the after-effects of cTBS and iTBS, analyses of latent variables showed that the effect of pre-SMA inhibition (by cTBS) on decision thresholds (increased a) continued ($p(a_{\text{inhibition}} > a_{\text{control}}) = .9990$), whereas there was now no significant effect of pre-SMA excitation (by iTBS) on the same parameter ($p(a_{\text{excitation}} > a_{\text{control}}) = .6194$) during the remaining test blocks. We observed significantly higher drift rates in the preSMA inhibition condition ($p(\nu_{\text{inhibition}} > \nu_{\text{control}}) = .9988$), whereas consistent with our primary analysis summarized above, there was no effect of pre-SMA excitation on drift rates ($p(\nu_{\text{excitation}} < \nu_{\text{control}}) = .6566$). Finally, non-decision times were significantly lower in both pre-SMA inhibition ($p(t_{\text{inhibition}} < t_{\text{control}}) = 1$) and excitation ($p(t_{\text{excitation}} < t_{\text{control}}) = .9993$) conditions.

5. Discussion

The current study investigated the causal role of right pre-SMA in modulating speed-accuracy tradeoff in choice behavior by testing the effects of both inhibition and excitation of pre-SMA on decision-threshold modulation. To this end, we applied non-invasive brain stimulation to right pre-SMA (cTBS for inhibition and iTBS for excitation) and vertex through using structural MRI-guided neuronavigation, and compared the DDM-based decision thresholds, as the latent variable of interest, across these three conditions in a within-subject design. Based on the cortico-striatal theory of SAT, we predicted decision thresholds to increase with the inhibition of pre-SMA and to decrease with the excitation of pre-SMA in comparison to vertex stimulation. Our results confirmed both of these predictions, both replicating our previous findings regarding the effect of pre-SMA inhibition on decision thresholds (Tosun et al., 2017) using more precise localization, and also providing a more complete empirical test of the cortico-striatal theory of SAT by testing for bi-directionality of this modulatory effect. Note that similar to the results of a number of previous studies (Erhan and Balcı, 2017; Forstmann and Wagenmakers, 2015; Georgiev et al., 2016; Tosun et al., 2017; Voss et al., 2004, 2013), these effects were observed in the absence of detectable effects at the level of behavioral outputs (i.e., accuracy or RT). We think that the mere possibility of having such dissociations demonstrates the value of computational approaches to decision-making particularly in elucidating its neural basis.

Within the framework of the striatal theory of SAT, the observed effects of pre-SMA stimulation on decision-threshold modulation in our study can be interpreted in terms of the downstream effects of our manipulations on striatal excitability. According to this theory, increase in pre-SMA activity would excite striatum, which in turn would decrease the inhibitory effect of basal ganglia on motor execution-related cortical areas (Forstmann et al., 2008). On the other side of the coin, decreased pre-SMA activity would decrease striatal excitability, bolstering the inhibitory effect of basal ganglia over its cortical efferents (Bogacz et al., 2010; Forstmann et al., 2008). These neural mechanisms would effectively correspond to narrower and wider decision thresholds, respectively (Forstmann et al., 2008, 2010 - see Figs. 1 and 5 for graphical depiction of these effects).

This interpretation is supported by Watanabe et al. (2015) who showed that the connectivity of pre-SMA and striatum, and striatum and globus pallidus interna were affected by the stimulation of pre-SMA pointing at the functional interaction between these regions at least in relation to response inhibition. It is also possible that the effects induced by the modulation of pre-SMA activity were mediated via the resultant effects on other brain regions such as the ipsilateral inferior-frontal cortex (e.g., Leisman et al., 2012; Xu et al., 2016). Future studies can target other regions that have been shown to be functionally connected with right pre-SMA to examine their role in the modulation of SAT in 2AFC tasks.

Our findings do not support the sub-thalamic nucleus (STN) theory of SAT since according to this approach inhibition of pre-SMA would decrease the STN activity and thus downregulate the inhibitory effect of basal ganglia on motor execution-related cortical efferents. According to this theory, excitation (and inhibition) of pre-SMA would result in the opposite effects on motor execution-related cortical areas by exciting (and not exciting) STN (Aron et al., 2007; Aron and Poldrack, 2006). Our results regarding decision thresholds constitute the exact opposite of what would result from these predictions (see Bogacz et al., 2010 for a critical review of different theories of SAT and their predictions).

Finally, the implication of our findings for the cortical theory of SAT is equivocal. Cortical theory asserts that SAT modulation is achieved through the baseline activity of cortical integrator neural populations. When the baseline activity is high the distance that needs to be traveled to reach a given threshold would be shorter, leading to fast but error prone decisions again due to random noise in evidence accumulation process. On the other hand, when the baseline activity is low, this distance to be traveled before making a decision would be higher, leading to slow but more accurate decisions. Thus, if right pre-SMA contains integrator neurons, our results might very well be explained also by the cortical theory of SAT. Different theories of SAT are illustrated in Fig. 5.

The current study expands on our previous work (Tosun et al., 2017) by replicating the finding that pre-SMA inhibition leads to higher

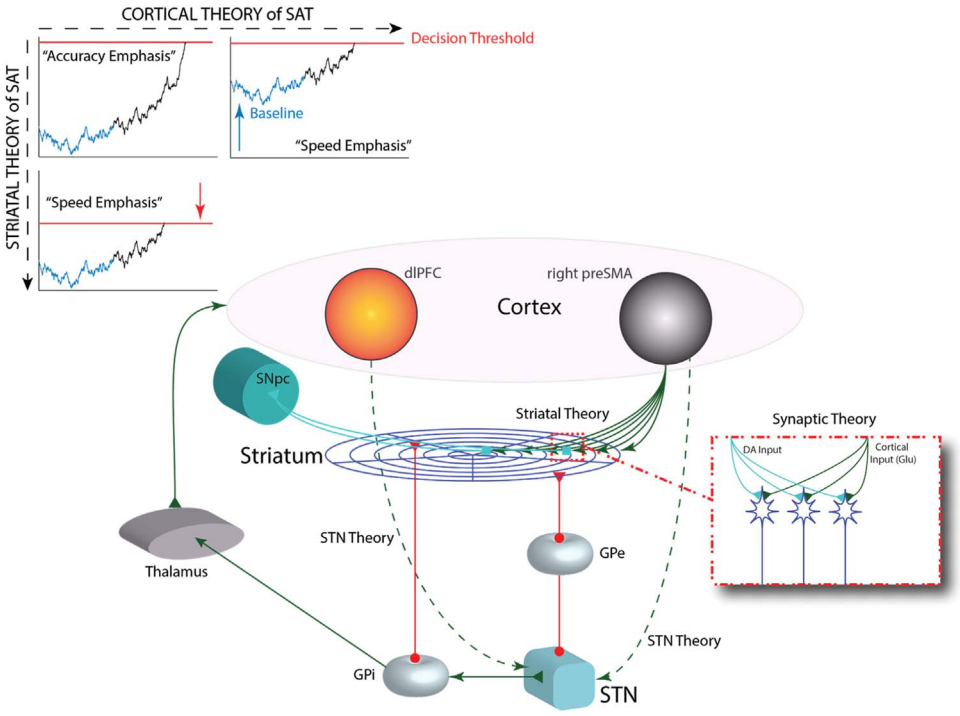

Fig. 5. Depiction of striatal, cortical, STN, and synaptic theories of SAT. Striatal theory is depicted by the primary excitatory projections of right pre-SMA on striatum and thereby the modulation of striatal excitability. The cortical theory and the striatal theory are depicted in terms of their core assumptions regarding the dynamics of the decision processes (top left panels). The comparison of cortical and striatal theories in terms of decision process (top left three panels) is inspired by Fig. 2 of Bogacz et al. (2010). The STN theory is depicted in terms of excitatory projections of dlPFC and pre-SMA onto STN. Finally, for completeness the synaptic theory is depicted in the rectangular zoom-in on striatal synapses (not described in main text but referred to here). According to this theory, SAT can be modulated by changing the efficacy of cortico-striatal synapses and thereby changing the sensitivity of striatal neurons to the cortical inputs through processes such as dopamine-dependent long-term potentiation (Lo & Wang, 2010). According to this view, long-term depression would effectively increase whereas long-term potentiation would effectively decrease the decision thresholds.

threshold setting and also showing that excitation of pre-SMA reduces the decision thresholds confirming the primary prediction of the cortico-striatal theory of SAT in both directions (i.e., increase and decrease) in a comprehensive fashion.

Although the direction of the pre-SMA inhibition on drift-rate was consistent with Tosun et al. (2017) and the effect of pre-SMA excitation was in the opposite direction, these effects were not statistically reliable for the first half of the data. This could be due to the fact that different from the previous study, we analyzed the data gathered from a shorter test period for the data to be comparable between cTBS and iTBS conditions while in the previous study the entire test session (due to much longer effect period of cTBS) was included in the analysis. Consistent with the findings of Tosun et al. (2017) however, cTBS led to higher drift-rates during the remaining test trials. Interestingly, there was no effect of iTBS on the drift rate during the corresponding test period. These findings suggest that the effect of the inhibition of preSMA on drift-rate is delayed compared to its effect on the decision-threshold setting. Further studies are required to elucidate the mechanisms that are affected in relation to drift-rates in 2AFC.

Acknowledgments

This study was supported by TÜBA (Turkish Academy of Sciences)-GEBİP 2015 award to F.B.

References

Aron, A.R., Poldrack, R.A., 2006. Cortical and subcortical contributions to stop signal response inhibition: role of the subthalamic nucleus. J. Neurosci. 26, 2424–2433.
Aron, A.R., Behrens, T.E., Smith, S., Frank, M.J., Poldrack, R.A., 2007. Triangulating a cognitive control network using diffusion-weighted magnetic resonance imaging (MRI) and functional MRI. J. Neurosci. 27 (14), 3743–3752. http://dx.doi.org/10.1523/JNEUROSCI.0519-07.2007.
Bogacz, R., 2007. Optimal decision-making theories: linking neurobiology with behaviour. Trends Cogn. Sci. 11, 118–125.
Bogacz, R., Gurney, K., 2007. The basal ganglia and cortex implement optimal decision making between alternative actions. Neural Comput. 19, 442–477.
Bogacz, R., Wagenmakers, E.J., Forstmann, B.U., Nieuwenhuis, S., 2010. The neural basis of the speed–accuracy tradeoff. Trends Neurosci. 33, 10–16.
Brainard, D.H., 1997. The psychophysics toolbox. Spat. Vision. 10, 433–436.
de Hollander, G., Labruna, L., Sellaro, R., Trutti, A., Colzato, L., Ratcliff, R., Ivry, R., Forstmann, B.U., 2016. Transcranial direct current stimulation does not influence the speed-accuracy tradeoff in perceptual decision making: Evidence from three independent replication studies. J. Cogn. Neurosci. 9, 1283–1294. http://dx.doi.org/10.1162/jocn_a_00967.
Ding, L., Gold, J.I., 2010. Caudate encodes multiple computations for perceptual decisions. J. Neurosci. 30, 15747–15759.
Erhan, C., Balcı, F., 2017. Obsessive compulsive features predict cautious decision strategies. Q. J. Exp. Psychol. 70 (1), 179–190. http://dx.doi.org/10.1016/j.jad.2016.09.011.
Forstmann, B.U., Wagenmakers, E.J., 2015. Model-based cognitive neuroscience: a conceptual introduction. In: Forstman, B.U., Wagenmakers, E.J. (Eds.), An introduction to model-based cognitive neuroscience. Springer, New York, pp. 139–156.
Forstmann, B.U., Anwander, A., Schäfer, A., Neumann, J., Brown, S., Wagenmakers, E.J., Bogacz, R., Turner, R., 2010. Cortico-striatal connections predict control over speed and accuracy in perceptual decision making. Proc. Natl. Acad. Sci. USA 107 (15916-4920).
Forstmann, B.U., Dutilh, G., Brown, S., Neumann, J., Von Cramon, D.Y., Ridderinkhof, K.R., Wagenmakers, E.J., 2008. Striatum and pre-SMA facilitate decision-making under time pressure. Proc. Natl. Acad. Sci. USA 105, 17538–17542.
Frank, M.J., 2006. Hold your horses: a dynamic computational role for the subthalamic nucleus in decision making. Neural Netw. 19, 1120–1136.
Georgiev, D., Rocchi, L., Tocco, P., Speekenbrink, M., Rothwell, J.C., Jahanshahi, M., 2016. Continuous theta burst stimulation over the dorsolateral prefrontal cortex and the pre-sma alter drift rate and response thresholds respectively during perceptual decision-making. Brain Stimul. 9 (4), 601–608. http://dx.doi.org/10.1016/j.brs.2016.04.004.
Gold, J.I., Shadlen, M.N., 2007. The neural basis of decision making. Annu. Rev. Neurosci. 30, 535–574.
Gold, J.I., Shadlen, M.N., 2001. Neural computations that underlie decisions about sensory stimuli. Trends Cogn. Sci. 5 (1), 10–16 (doi:0.1016/S1364-6613)(00)(01567-9).
Gurney, K., Prescott, T.J., Wickens, J.R., Redgrave, P., 2004. Computational models of the basal ganglia: from robots to membranes. Trends Neurosci. 27, 453–459.
Hartwigsen, G., Bergmann, T.O., Herz, D.M., Angstmann, S., Karabanov, A., Raffin, E., Thielscher, A., Siebner, H.R., 2015. Modeling the effects of noninvasive transcranial brain stimulation at the biophysical, network, and cognitive level. Progress. brain Res. 222, 261–287.
Herz, D.M., Tan, H., Brittain, J.S., Fischer, P., Cheeran, B., Green, A.L., Foltynie, T., 2017. Distinct mechanisms mediate speed-accuracy adjustments in cortico-subthalamic networks. Elife 6, e21481.
Huang, Y.Z., Edwards, M.J., Rounis, E., Bhatia, K.P., Rothwell, J.C., 2005. Theta burst stimulation of the human motor cortex. Neuron 45 (2), 201–206.
Ivanoff, J., Branning, P., Marois, R., 2008. fMRI evidence for a dual process account of the speed-accuracy tradeoff in decision-making. PLoS One 3, e2635.
Kadosh, R.C., Muggleton, N., Silvanto, J., Walsh, V., 2010. Double dissociation of format-dependent and number-specific neurons in human parietal cortex. Cereb. Cortex 20 (9), 2166–2171.
Leisman, G., Melillo, R., Carrick, F.R., 2012. Clinical motor and cognitive neurobehavioral relationships in the basal ganglia. In: Fernando, A.F.A., Barrios Bauer, C. (Eds.), Basal Ganglia: An Integrative View. Intech, Rijeka, Croatia, pp. 1–30.
Lo, C.C., Wang, X.J., 2006. Cortico–basal ganglia circuit mechanism for a decision threshold in reaction time tasks. Nat. Neurosci. 9, 956–963.

Mansfield, E.L., Karayanidis, F., Jamadar, S., Heathcote, A., Forstmann, B.U., 2011. Adjustments of response threshold during task switching: a model-based functional magnetic resonance imaging study. J. Neurosci. 31, 14688–14692.
Matzke, D., Wagenmakers, E.J., 2009. Psychological interpretation of the ex-Gaussian and shifted Wald parameters: a diffusion model analysis. Psychon. Bull. Rev. 16 (5), 798–817. http://dx.doi.org/10.3758/PBR.16.5.798.
Pelli, D.G., 1997. The VideoToolbox software for visual psychophysics: transforming numbers into movies. Spat. Vision. 10, 437–442.
Raftery, A.E., 1995. Bayesian model selection in social research. Sociol. Methodol. 25, 111–164.
Ratcliff, R., 1978. A theory of memory retrieval. Psychol. Rev. 85, 59–108.
Ratcliff, R., McKoon, G., 2008. The diffusion decision model: theory and data for two-choice decision tasks. Neural Comput. 20, 873–922.
Ratcliff, R., Rouder, J.N., 1998. Modeling response times for two-choice decisions. Psychol. Sci. 9, 347–356.
Ratcliff, R., Smith, P.L., 2004. A comparison of sequential sampling models for two-choice reaction time. Psychol. Rev. 111 (2), 333.
Sack, A.T., Kadosh, R.C., Schuhmann, T., Moerel, M., Walsh, V., Goebel, R., 2009. Optimizing functional accuracy of TMS in cognitive studies: a comparison of methods. J. Cogn. Neurosci. 21 (2), 207–221.
Schouten, J.F., Bekker, J.A.M., 1967. Reaction time and accuracy. Acta Psychol. 27, 143–153.
Shadlen, M.N., Newsome, W.T., 2001. Neural basis of a perceptual decision in the parietal cortex (area LIP) of the rhesus monkey. J. Neurophysiol. 86, 1916–1936.
Smith, P.L., Ratcliff, R., 2004. Psychology and neurobiology of simple decisions. Trends Neurosci. 27, 161–168.
Soto, D., Llewelyn, D., Silvanto, J., 2012. Distinct causal mechanisms of attentional guidance by working memory and repetition priming in early visual cortex. J. Neurosci. 32 (10), 3447–3452.
Tosun, T., Berkay, D., Sack, A.T., Çakmak, Y.Ö., Balcı, F., 2017. Inhibition of Pre-SMA by Continuous Theta Burst Stimulation Leads to More Cautious Decision-making and More Efficient Sensory Evidence Integration. J. Cogn. Neurosci. http://dx.doi.org/10.1162/jocn_a_01134.
van Maanen, L., Brown, S.D., Eichele, T., Wagenmakers, E.J., Ho, T., Serences, J., Forstmann, B.U., 2011. Neural correlates of trial-to-trial fluctuations in response caution. J. Neurosci. 31 (48), 17488–17495.
van Veen, V., Krug, M.K., Carter, C.S., 2008. The neural and computational basis of controlled speed-accuracy tradeoff during task performance. J. Cogn. Neurosci. 20, 1952–1965.
Voss, A., Nagler, M., Lerche, V., 2013. Diffusion models in experimental psychology. Exp. Psychol. 60 (6), 385–402. http://dx.doi.org/10.1027/1618-3169/a000218.
Voss, A., Rothermund, K., Voss, J., 2004. Interpreting the parameters of the diffusion model: an empirical validation. Mem. Cogn. 32 (7), 1206–1220. http://dx.doi.org/10.3758/BF03196893.
Wagenmakers, E.J., Ratcliff, R., Gomez, P., McKoon, G., 2008. A diffusion model account of criterion shifts in the lexical decision task. J. Mem. Lang. 58 (1), 140–159.
Watanabe, T., Hanajima, R., Shirota, Y., Tsutsumi, R., Shimizu, T., Hayashi, T., et al., 2015. Effects of rTMS over pre-supplementary motor area on fronto-basal-ganglia network activity during stop-signal task. J. Neurosci. 35, 4813–4823.
Wenzlaff, H., Bauer, M., Maess, B., Heekeren, H.R., 2011. Neural characterization of the speed–accuracy tradeoff in a perceptual decision-making task. J. Neurosci. 31, 1254–1266.
Wickelgren, W.A., 1977. Speed-accuracy tradeoff and information processing dynamics. Actapsychologica 41, 67–85.
Wiecki, T.V., Sofer, I., Frank, M.J., 2013. HDDM: hierarchical bayesian estimation of the drift-diffusion model in python. Front. Neuroinformatics 7, 14.
Xu, B., Sandrini, M., Wang, W.T., Smith, J.F., Sarlls, J.E., Awosika, O., Cohen, L.G., 2016. PreSMA stimulation changes task-free functional connectivity in the fronto-basal-ganglia that correlates with response inhibition efficiency. Human. Brain Mapp. 37 (9), 3236–3249. http://dx.doi.org/10.1002/hbm.23236.